processes

MDPI

Review

Single-Molecule Chemical Reactions Unveiled in Molecular Junctions

Ian Bunker [1], Ridwan Tobi Ayinla [1] and Kun Wang [1,2,*]

[1] Department of Chemistry, Mississippi State University, Mississippi State, MS 39762, USA
[2] Department of Physics and Astronomy, Mississippi State University, Mississippi State, MS 39762, USA
* Correspondence: kw2504@msstate.edu

Abstract: Understanding chemical processes at the single-molecule scale represents the ultimate limit of analytical chemistry. Single-molecule detection techniques allow one to reveal the detailed dynamics and kinetics of a chemical reaction with unprecedented accuracy. It has also enabled the discoveries of new reaction pathways or intermediates/transition states that are inaccessible in conventional ensemble experiments, which is critical to elucidating their intrinsic mechanisms. Thanks to the rapid development of single-molecule junction (SMJ) techniques, detecting chemical reactions via monitoring the electrical current through single molecules has received an increasing amount of attention and has witnessed tremendous advances in recent years. Research efforts in this direction have opened a new route for probing chemical and physical processes with single-molecule precision. This review presents detailed advancements in probing single-molecule chemical reactions using SMJ techniques. We specifically highlight recent progress in investigating electric-field-driven reactions, reaction dynamics and kinetics, host–guest interactions, and redox reactions of different molecular systems. Finally, we discuss the potential of single-molecule detection using SMJs across various future applications.

Keywords: single-molecule detection; chemical reactions; molecular junctions; electrical detection

Citation: Bunker, I.; Ayinla, R.T.; Wang, K. Single-Molecule Chemical Reactions Unveiled in Molecular Junctions. *Processes* **2022**, *10*, 2574. https://doi.org/10.3390/pr10122574

Academic Editor: Suresh K. Bhatia

Received: 9 November 2022
Accepted: 28 November 2022
Published: 3 December 2022

1. Introduction

The ability to reveal the microscopic details of chemical reactions is essential for understanding and manipulating chemical, physical, and biological processes that can have a transformative impact on materials discovery, sustainability, and life science. Chemical reactions at the single-molecule level not only provide mechanistic insights of the reaction cascade and intermediates that are often difficult to access in bulk, but they are also critical for studying the reaction kinetics and dynamics and the microscopic effects of various stimuli. In conventional bulk chemical processes, chemists mostly rely on the statistical average of a large number of molecules to account for the individual behavior of molecules during chemical reactions [1,2]. In this approach, changes in reaction intermediates, product formation, and the concentration of reactants are considered a time-dependent equilibrium process. On the contrary, at the single-molecule level, researchers have the advantage of accessing the discrete nature of individual molecular species taking part in a chemical reaction [3,4]. This defined and specific access to controlled single molecular responses has the potential to unveil novel reaction pathways, identify commonly misjudged transient transition states, reveal specific molecular responses to different external stimuli, and provide chemists with an accurate prediction of reactant species [5,6]. The advent of several emerging single-molecule electrical detection techniques based on single-molecule junctions (SMJs), including the scanning tunneling microscope break junction (STMBJ) [7–9], conductive atomic force microscope (CAFM) [10,11], mechanically controlled break junction (MCBJ) [12,13], electron migration break junction (EMJ) [14,15], and graphene-molecule-graphene (GMG) [16–18] junctions, have made it possible to probe the intrinsic nature

of chemical species. Although the primary operational principles of these powerful techniques are different, they all project a central idea in detecting chemical reactions of single molecules trapped between two nanoelectrodes, i.e., relying on an electrical signal (current) to monitor the reaction progress [19–21]. This powerful detection method allows one to systematically investigate chemical processes with single-molecule precision, which is otherwise impossible.

Reacting chemicals at the single-molecule level has offered novel insights into fundamental reaction mechanisms [22–27]. By analyzing the interaction of reactants at the atomic scale, a unique perspective is provided on the mechanisms involved in product formation [28]. Interplaying factors, such as reactivity, reactants' orientations, the reaction environment, and external stimuli, determine the configuration and selectivity of the dominant product. If these conditions could be ingeniously manipulated, reactions could be guided in a drastically simplified and controlled manner. SMJs provide a unique platform for simultaneous investigation, manipulation, detection, and stimulation of chemical reactions [29]. As a result of nanoscale surface limitation which reduces the active binding site and specific alignment of the reaction axis, single-molecule chemical reactions cannot replace a traditional bulk chemical reaction [2,6]. However, the process of reacting chemical species in between the nanostructured electrodes has suggested how synthetic chemistry can be re-envisioned to meet the future advanced green chemistry.

Generally, there are two popularly adopted approaches when reacting chemicals using SMJ-based techniques. In the first approach, a reactant species is used to functionalize the end of an atomically sharp electrode while the other reactant species is chemisorbed on another electrode. A controlled and precise mechanical modulation is then applied to either of the two electrodes to approach both reactants to a distance that favors the reaction of both reactant species in the coordinate that favors product formation (Figure 1a). Under an applied external bias across the two reactant functionalized electrodes, bond formation between the two reactants can be detected by monitoring the electrical current flowing in the junction (e.g., repeatable and consistent current jumps and breakdown over time). Repeating the bond formation and bond breaking process through controlled and precise mechanical modulation causes the current to "blink" [30]. The blinking approach is time-dependent and most suitable for conducting reaction dynamics and catalysis. However, it has a low yield and requires high instrumental stability. The second approach takes advantage of an external stimulus (such as light, an oriented external electric field, electrochemical environment, etc.) applied to a traditional electrode-molecule-electrode junction to catalyze a bond formation or cleavage (Figure 1b). The single-molecule junction response to external stimulus is then observed as a function of the junction conductance change [31–33]. Recent studies using this method have focused on several key aspects of a reaction, including catalysis, isomerization, selectivity, and transient intermediate states at the single-molecule level [34,35]. In this review, we survey recent progress in studying stimuli-driven chemical reactions, reaction kinetics, and dynamics at the single-molecular level. Specifically, electric-field-driven reactions, reaction kinetics, host–guest interactions, and redox reactions explored using SMJ devices are highlighted. To this end, significant attention is given to recent experimental investigations and relevant historical discoveries within single-molecule research. We also discuss the potential of SMJ techniques in future investigations of chemical processes.

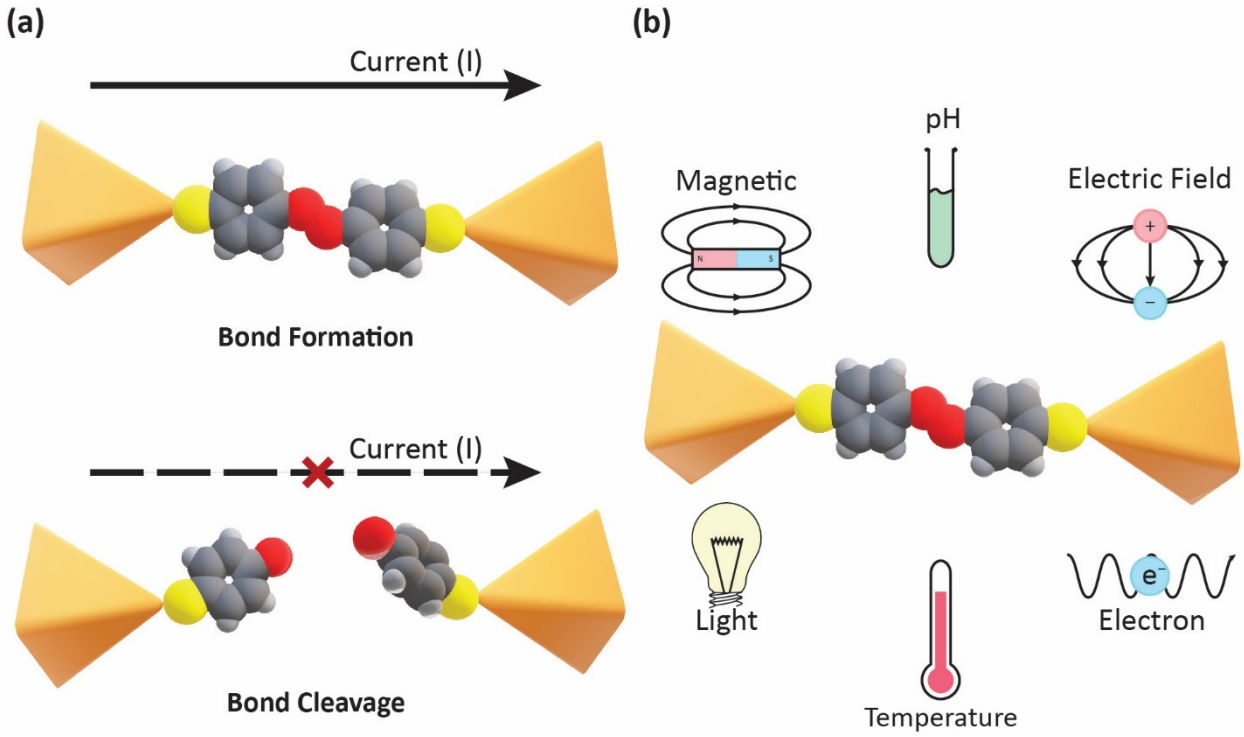

Figure 1. Probing a chemical reaction at the single-molecule level: (**a**) schematic illustration of bond formation and cleavage; (**b**) stimuli-induced chemical reaction.

2. Electric-Field-Driven Chemical Reactions

For many years, an oriented external electric field (OEEF) has been theoretically projected as an active and smart reagent for chemical reaction selectivity, isomerization, and catalysis [36]. Directing EEF along the coordinate of the reaction pathway has the potential to lower energy barriers and manipulate resonance stability, further driving chemical reactions [37]. Recently, this theoretical promise has witnessed a profound experimental breakthrough at the single-molecule scale, thanks to the promising SMJ technique. In the presence of an electric field, reacting species can undergo several known phenomena: (a) the Stark effect—which explains the shifting and/or splitting of the spectra lines of discrete molecules or atoms when exposed to an OEEF [38–40]. (b) Zwitterionic state stabilization—OEEF directly impacts the stability of charge-separated zwitterionic states by lowering the energy of the transition states; this stabilization effect helps to monitor the transient ionic species as the reaction progress [41]. (c) Bond cleavage—orienting an electric field in the reaction axis has the potential to polarize the bonds in the reaction coordinate which eventually causes heterolytic bond cleavage [42]. (d) Selectivity—OEEF has also been established to selectively catalyze chemical reactions by favoring the formation of specific product against another [36,43]. In 2016, Aragonè et al. used an external electric field oriented in the reaction axis of single molecules of diene attached to a Au tip and a dienophile attached to a Au flat substrate to catalyze a Diels–Alder reaction (Figure 2a) using a STM setup [30]. They studied the effect of electric field orientation by monitoring the reaction rate using the blinking STM experiment. A five-time increase in the reaction rate was observed when the electric field was aligned to favor the movement of electrons from the dienophile to the diene (Figure 2b).

Zang et al. also explored the efficacy of an electric field in catalyzing an isomerization reaction of cumulene[3] derivatives [44]. They used STM as the source of a large external electric field to induce selective isomerization of Cis[3] to Trans[3] cumulene in the break-junction scheme. In their experiment, they first determined the conductance signature of Cis[3] and Trans[3] isomers independently. The conductance signature of the Cis[3] isomer was found to be broad with a short conductance plateau whose length is approximately

equal to the length (0.84 nm) of the Cis[3] isomer, while the conductance signature of the Trans[3] isomer is distinct, with a slightly higher conductance whose length is also comparable to the length (1.44 nm) of the Trans[3] isomer. They followed up by measuring the conductance of the Cis[3] isomer over the span of 32 h in the presence of an electric field and observed a steady isomerization of the Cis[3] to Trans[3] isomer owing to the transformation of the Cis[3] conductance plateau to the Trans conductance plateau.

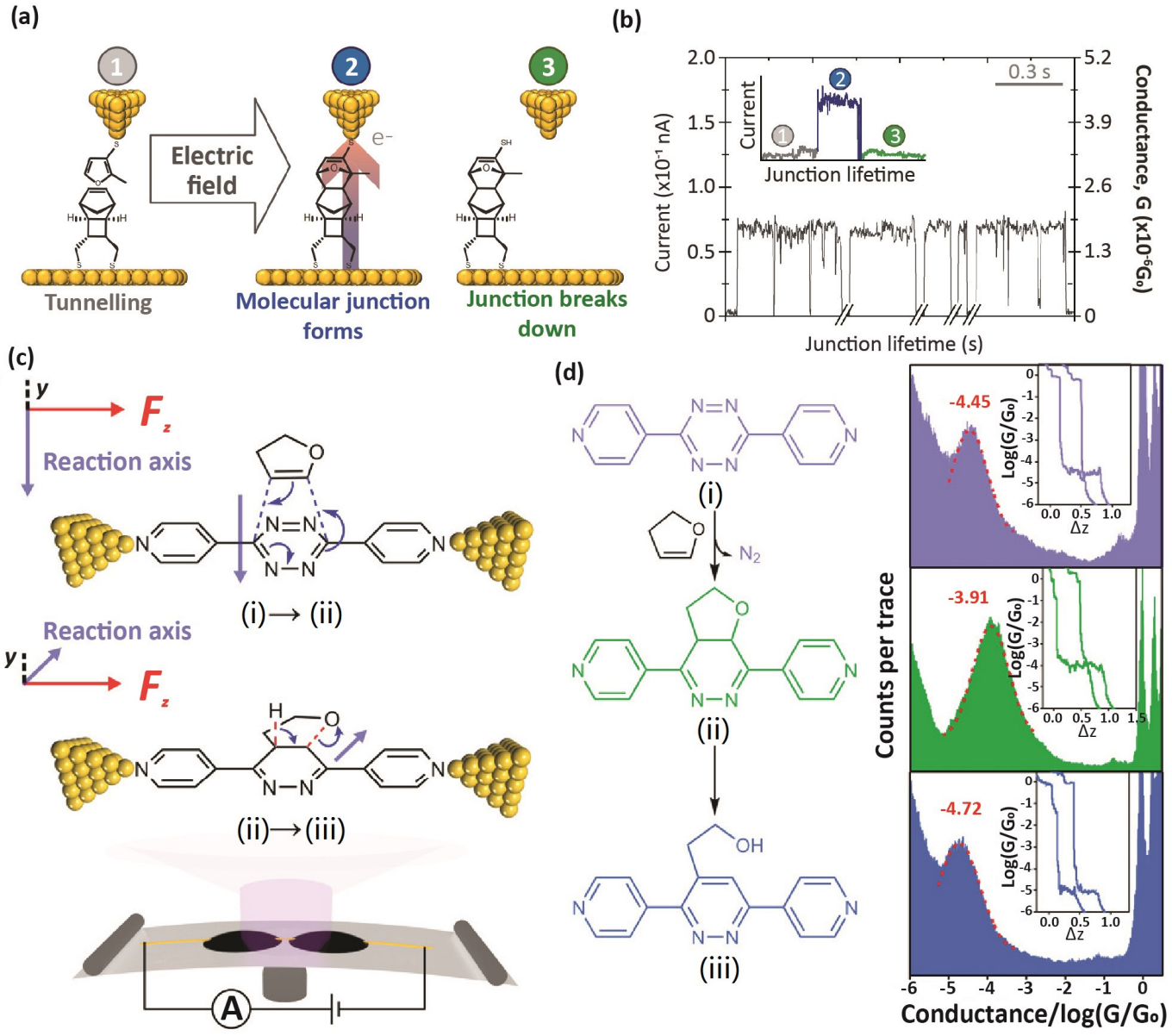

Figure 2. Electric-field-driven Diels–Alder reaction (**a**) Schematics of the STM tip approach and retract stages of the blinking junction. Label 1 corresponds to a diene and a dienophile reactant attached to a Au tip and substrate before reaction, 2 corresponds to the product of the reaction in 1, and 3 corresponds to the retraction stage where the junction breaks down. (**b**) The real-time current signal of the Diels–Alder reaction shown in (**a**). The inset corresponds to an arbitrary trace of 1, 2, and 3. Figures were reproduced with permission from reference [30]. Copyright 2016, Springer Nature. (**c**) A single-molecule Diels–Alder reaction in MCBJ. The direction of the electric field, F_z (red arrow), is orthogonal to the reaction axis (blue arrow) and parallel to the *y*-axis. (**d**) Stages of the Diels–Alder reaction and their corresponding conductance plateau: (**i**) ($10^{-4.45}$ G_0) corresponds to the reaction of furan and a dienophile to form (**ii**) ($10^{-3.91}$ G_0), which also forms (**iii**) ($10^{-4.72}$ G_0) after aromatization. Figures were reproduced with permission from reference [45]. Copyright 2019, Science Advances.

In another experiment, Huang et al. used localized electric field alignment to selectively catalyze the two cascade stages of a Diels–Alder reaction followed by an aromatization reaction using MCBJ technique [45]. As shown in Figure 2c, F_z is the direction of the electric field which is orthogonal to the reaction axis. They observed that the OEEF selectively accelerates the aromatization reaction by a one order of magnitude increase in the reaction rate. In Figure 2d, the single-molecule conductance corresponding to each reaction state denoted by (i) is $10^{-4.45}$ G_0, (ii) is $10^{-3.91}$ G_0, and (iii) is $10^{-4.72}$ G_0. This result represents an elegant breakthrough in experimentally showcasing the role of an OEEF in a selective catalytic process at the single-molecule level.

3. Reaction Dynamics and Kinetics in Single-Molecule Junctions

Synthetic chemists are often challenged with answering key questions about (i) how do chemical reactions occur? (ii) At what time scale do reactant species undergo chemical changes? (iii) What are the intermediate states of the reactant species undergoing a chemical reaction? Emerging intermediate chemistry also seeks the possibility of trapping intermediate species as an active precursor for secondary reactions. Thorough understanding of a chemical process requires in-depth investigation of both the dynamics and kinetics of a chemical reaction. While reaction dynamics focus on the mechanism of chemical changes while accounting for the drive causing the change, kinetics study concerns the rate at which the chemical transformation occurs (i.e., standard measure of the frequency at which reactant species undergo chemical changes) [2,6]. Careless observation of bulk reaction processes may potentially create ambiguity or misinterpretation, and consequently leads to misinformation of key reaction processes. One unique advantage of single-molecule investigation is that it enables direct tracking of the time trajectory of reaction pathways, which helps to unveil the molecular geometry of intermediates/transient states that are often inaccessible in ensemble measurements [46,47]. For instance, Guan et al. reported a solvent-dependent nucleophilic addition reaction of hydroxylamine to carbonyl at the single-molecule level using the GMG junction (Figure 3a) [48]. They covalently bonded a 9-fluorenone functional center in between two graphene electrodes to form a GMG junction while unambiguously tracking the corresponding electrical signals associated with the reaction states. Figure 3b shows the reversible solvent-dependent bimodal real-time current profile of the addition reaction dynamics of the mixture of EtOH/H_2O with NH_2OH and NaOH. Beyond the fundamental addition reaction chemistry, their work showed that intermediate states can react with remains of reactant species at a high time scale in different solvent environments. Their idea has opened a new route in using intermediate states as in situ reagents in chemical process. In another work, Zhou et al. reported the dynamics of hydrogen bonds with single-bond resolution [49]. They covalently bound a quadrupolar hydrogen system in between graphene electrodes to form a stable GMG junction to probe the dynamics of an individual hydrogen bond at different temperatures and in various solvents. They showed a multimodal distribution of current signals as a result of the random rearrangement of hydrogen bond structures through an intermolecular proton transfer. Given the extreme difficulty in the direct observation of hydrogen bond dynamics, their results further reestablished the ultimate resolution of break junction technique by deciphering proton transfer dynamics at the single-molecule scale.

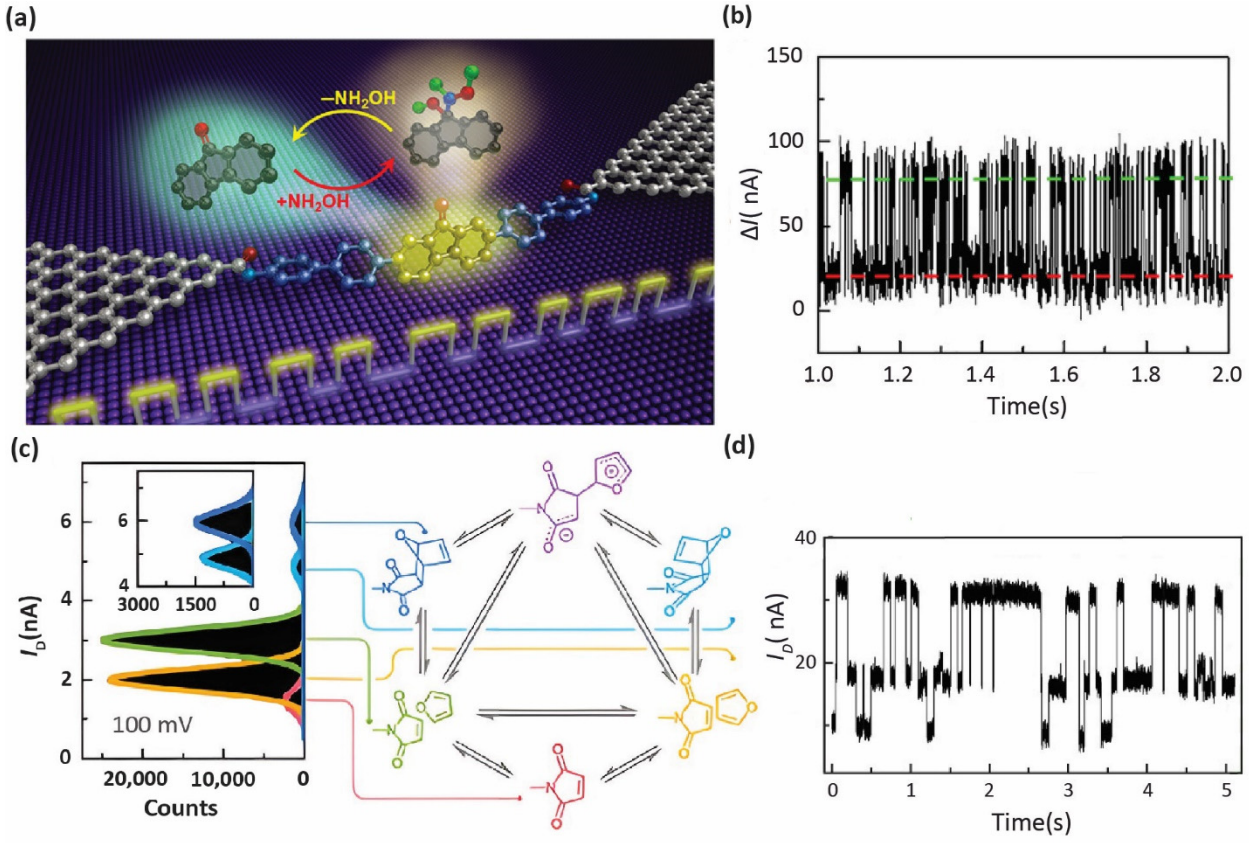

Figure 3. Reaction dynamics in SMJs. (**a**) Schematic representation of a reversible nucleophilic addition reaction of hydroxylamine to carbonyl. (**b**) Bimodal real-time current signals of a nucleophilic addition reaction. Figures were reproduced with permission from reference [48]. Copyright 2018, Science Advances. (**c**) Multiple conductance states corresponding to several intermediate states in a Diels–Alder reaction mechanism at 100 mV. (**d**) Multimodal real-time current signal. Figures were reproduced with permission from reference [50]. Copyright 2021, Science Advances.

Recently, Yang et al. took advantage of the high stability and temporal resolution of the GMG junction to unveil an unprecedented time trajectory of the Diels–Alder reaction under a high electric field [50]. They used electric current signals to distinguish five different zwitterionic intermediate states and their time scales (Figure 3c,d). The Diels–Alder reaction is considered "concerted" (all bond formations and breaking are mechanistic but in a single step); therefore, the time scale of the intermediate states is faster than the response of many conventional spectroscopy techniques. They also reacted maleimide with furan while changing the orientation of the external electric field and observed that orienting the electric field along the line connecting the partial charge delayed the transition structure. Jia et al. designed a reversible photo-switch by covalently trapping a single molecule of light-sensitive diarylethene in the nano-space of two graphene electrodes [51]. The original form of the molecule is insulating and denoted as being open form. In the GMG junction, they varied the wavelength of light to excite electrons in the molecule, which induced reversible switching of the current signals with a high on/off ratio.

Understanding the Suzuki–Miyaura coupling has witnessed tremendous attention from organic and organometallic chemists because of its mild reaction condition, ecological friendliness, availability of common boronic acid, and ultimately, it offers a reliable means of preparing a wide range of organic compounds using natural precursors [52–54]. However, despite this great attention, the full reaction pathway and specific reaction intermediate of Suzuki–Miyaura coupling remain elusive [55–57]. Contrary to the conventional analytical techniques that rely on taking averages of an ensemble to characterize the unstable fleeting intermediates, Yang et al. cleverly deployed label-free, high resolution, non-destructive,

single-molecule junctions to monitor and unveil the full pathway and reaction intermediate of Suzuki–Miyaura coupling [58]. They covalently bound a single molecule of palladium catalyst between a nanogap of graphene electrodes. They reported distinct, sequential, and periodic electrical signals emanating from oxidative addition/ligand exchange, pretransmetallation, transmetallation, and reductive elimination. The periodic cycles comprised of three conductance states were revealed. The first conductance state corresponds to oxidative addition followed by an instantaneous ligand exchange that was not observable in the bulk catalytic process due to its short lifetime. After the first step, successive second and third conductance plateaus followed which translate to the transition from the ion exchange to the pretransmetallation and transmetallation stages. The results of their work decoupled the ambiguity in the Suzuki–Miyaura cross-coupling and clarified that ion exchange is a transient state that precedes the rate-dependent transmetallation step. A clear understanding of the specific reaction pathway and time trajectory of the intermediate stages of reactions is key to fostering the design of highly efficient and economical catalytic processes.

4. Host–Guest Interactions

In 1987, the Nobel prize in chemistry was awarded to Donald J. Cram, Jean-Marie Lehn, and Charles J. Pedersen for their landmark achievement in the development of a structure-specific assembly of molecules motivated by noncovalent interactions of defined selectivity called the "Host–Guest" systems [59,60]. Since then, research into the host–guest systems has become increasingly popular among chemists, physicists, advanced material scientists, and biologists as applied to drug delivery, nanomedicine, molecular electronics, sensors and actuators, catalysis, functional materials, and so on [61–65]. Simple and complex supramolecular structures can be assembled when a "host" (macrocycles) molecule accommodates another "guest" molecule through any form of noncovalent interactions like π-π interaction, van der Waals interaction, electrostatic interactions, hydrophobic/hydrophilic interactions, and hydrogen bonding [66]. It has been shown that the robust SMJ techniques can also account for weak noncovalent interactions between the host and guest molecules [1]. For example, Milan et al. formed a host–guest complex in an STMBJ setup by rotaxinating an unstable archetypical insulating hexayne with a macrocycle (Figure 4a) [67]. They attached a 3,5-diphenylpyridine on either side of the hexayne molecular wire to serve as a stopper for the mobile macrocycle and an anchor for the Au electrodes. The molecular conductance of both the molecular wire and the host–guest assembly revealed that the mobile macrocycle does not significantly affect the conductance profile of the hexayne molecule (Figure 4b). To further establish the sensitivity (extreme limit of detection), Yuan et al. compared and reported the kinetics of a dimerization reaction of a cucurbit [8] molecule hosting a 1,2-bis(4-pyridinyl)ethylene guest using an in situ STMBJ and nuclear magnetic resonance (NMR) [68]. In NMR, the characteristic peaks of the reactants are not noticeable because of the small reactant concentrations; however, clear and defined electrical signals are noticeable and detected in STMBJ for reactant concentrations that are as low as 5×10^{-6} M. They also reported that a strong electric field in the nanogap increased the efficiency of host–guest formation. Zhang et al. also used cucurbit[8]uril as a host molecule to recreate the environment of different conformations of viologen (bipyridinium) guest molecules as shown in Figure 4c [69]. They recorded the conductance profile of each viologen conformation with their corresponding viologen guest. Their results show a significant increase in conductance when a cucurbit[8] molecule hosts the viologen guest molecule (Figure 4c).

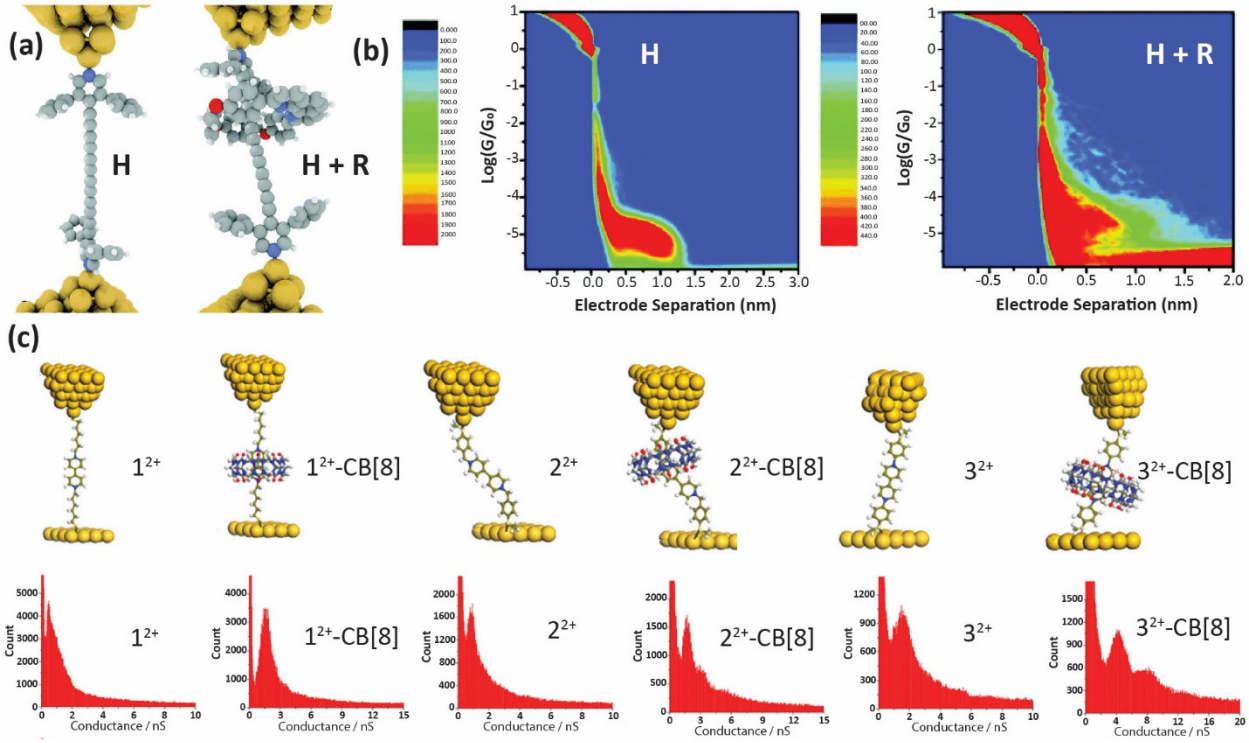

Figure 4. Host–guest interactions in single-molecule junctions. (**a**) Schematic representation of a guest hexayne dumbbell (H) and a hexayne-rotaxane complex (H + R). (**b**) Two-dimensional conductance histogram of H and H + R. Figures were reproduced with permission from reference [67]. Copyright 2017, Royal Society of Chemistry. (**c**) Illustration of different conformations of viologen guests and their cucurbit[8]uril host (top) with their corresponding 1-D conductance profile (bottom). Figures were reproduced with permission from reference [69]. Copyright 2016, American Chemical Society.

5. Redox Reaction

A reduction and oxidation (redox) reaction involves the simultaneous transfer of electron(s) between chemical species (atoms, ions, molecules) taking part in a chemical reaction [70]. Due to the ubiquitous nature of redox reactions in many important areas, such as corrosion, catalysis, combustion, and photosynthesis, understanding the details of mechanistic processes of redox reactions and the rationalization of previously unknown electron and proton transfer phenomena of single molecules in electrochemical systems has attracted significant attention in recent years [71,72]. To this end, one of the productive foregoing directions is to explore the synergistic advantage of electrochemistry and the diverse capability of SMJ techniques to address key questions on redox reactions at the single-molecule level [73,74]. Charge transport in SMJ is often dominated by either coherent tunneling or incoherent hopping. Coherent tunneling is a phase retention, single-step process where the molecular core behaves as a scatterer. The Landauer formalism accurately predicts a zero-bias conductance $G = G_0 T(E_F)$, where quantum conductance $G_0 = 2e^2/h = 77.8$ μS, and $T(E_F)$ is the transmission function of electrons at the Fermi energy of electrode E_F. In an electrolytic environment, where the molecular core is undergoing a redox reaction by an electrochemical potential, the $T(E_F)$ changes [75,76]. This change alters the electron transmission efficiency of the system, resulting in a sudden current change around the electrochemical equilibrium potential of the molecule undergoing the redox reaction. In this regime, plotting the electrochemical response of the redox molecule against the conductance shows a sigmoidal shape at the center which connotes the potential at which the redox transition takes place [77–79]. Incoherent hopping, on the other hand, is considered a combination of multiple-step transport processes, with the molecular core accepting and releasing charges for a non-zero time. When a redox-active molecule is used as a hopping site for charges, the mechanism of the charge transport is semi-classical based on the

Marcus theory with multiple rate constants [80,81]. A redox reaction occurs when a single electron travels from the source electrode to the drain electrode, leading to a rearrangement of the reaction energetics of the entire redox cell to accommodate the cascade electron-hopping processes [73,79]. The shift in the reaction energetics results in an enhancement of the charge transport efficiency at the equilibrium potential. Contrary to the sigmoidal-shaped signature of the conductance vs. electrochemical potential of the coherent tunneling transport, the incoherent hopping transport of redox-active molecules is bell-shaped with its maximum at the transition potential [82,83].

Several open and closed shell redox-active moieties, including benzodifuran [72], diazonium [84], metalloproteins [85–87], coronene [88], bipyridinium [79,83], anthraquinones [89], Cucurbit[n]uril [74], polyoxometalate [90], viologen [89], perylene tetracarboxylic acid [91–93], ferrocene [94], etc., have been studied at the single-molecule level by sweeping potentials in an electrochemical cell. For instance, Li et al. tuned the charge transport of a redox-active single-molecule naphthalenediimide (ND) pendant flanked by a dihydrobenzothiophene anchor using an electrochemical STMBJ (Figure 5a) [95]. They took advantage of the wide potential window of the ionic liquid in the electrochemical cell to access three reversible distinct charge states with well-defined conductance plateaus (Figure 5b). During a potential sweep, they observed that the neutral state of ND showed a conductance 10^{-4} G_0 at -0.20 V which changed to $10^{-3.3}$ G_0 at -1.50 V upon reduction to the first anionic radical (ND^{1-}) state. At -1.50 V, the conductance also increased to $10^{-3.0}$ G_0 as a result of further reduction to the second anionic (ND^{2-}) state. In another experiment, Chen et al. added a positively charged electrostatic anchor formed from the Coulombic interaction between Au electrodes and positively charged pyridinium terminals to the existing anchor bank [96]. In their work, they also demonstrated redox switching sponsored by charge injection in neutral 4,4′-bipyridine (BIP), radical cationic bipyridine-methyl viologen (BIP-$Me^{\bullet+}$), and dicationic BIP-Me^{2+}. The conductance measurement in the three species shows two (low and high) distinct conductance plateaus. The low and high conductance states in the neutral state were attributed to the change in the contact geometry of the single-molecule junction during tip retraction. However, there is a significant increase in the bimodal conductance states of BIP-$Me^{\bullet+}$ and dicationic BIP-Me^{2+} traceable to the key role of the anchor group in electron injection and extraction. Recently, Naghibi et al. successfully incorporated single-molecule persistent 6-oxo-verdazyl radicals between the source and drain electrodes of STMBJ containing an electrochemical cell using a thioanisole anchor (Figure 5c) [97]. Prior cyclic voltammetry measurement showed that a reversible one-electron oxidation of the open shell structure of 6-oxo-verdazyl to a monocation at +0.36 V and a one-electron reduction to a monoanion at -1.03 V. To access the potential window of the redox molecule, electrochemical measurements were done in 1-butyl-3-methylimidazolium triflate ionic liquid. Between a -0.2 V to -0.8 V vs. Fc/Fc^{+} gate potential, a slight gating effect was observed with a small and slow stepwise conductance increase (Figure 5d). At -1 V vs. Fc/Fc^{+} (near the reduction potential of the open shell structure), a sudden and abrupt drop in conductance by almost one order of magnitude occurs and continues to decrease as the potential is further reduced. The result of their work highlighted the possibility of using an electrochemical cell to stabilize persistent radicals and further establish a fascinating route to incorporating open shell structures into molecular electronics. Yin et al. used an electrochemical cell to activate a redox reaction in [8,8′biindino]thiophenylidene (BTP) molecular wire (Figure 5e) [98]. At a positive gate potential, they recorded low values of conductance that depict that the charge transport is dominated by the highest occupied molecular orbital. At a negative potential bias, they observed a slight surge in the conductance until -1.4 V. At a negative bias below -1.4 V and a positive bias above 1 V, a significant and reversible switch in conductance was observed, which corresponds to the reversible oxidation and reduction of the BTP molecular center (Figure 5f). They cleverly leveraged Hückel's theory of antiaromaticity to show conductance switching in a redox active molecule. Clearly, the development of electrochemical break junction techniques is key to addressing reactions

involving redox-active molecules at the single-molecule level, and helps to create an ideal environment to stabilize and test anions, cations, and radicals that are otherwise unstable.

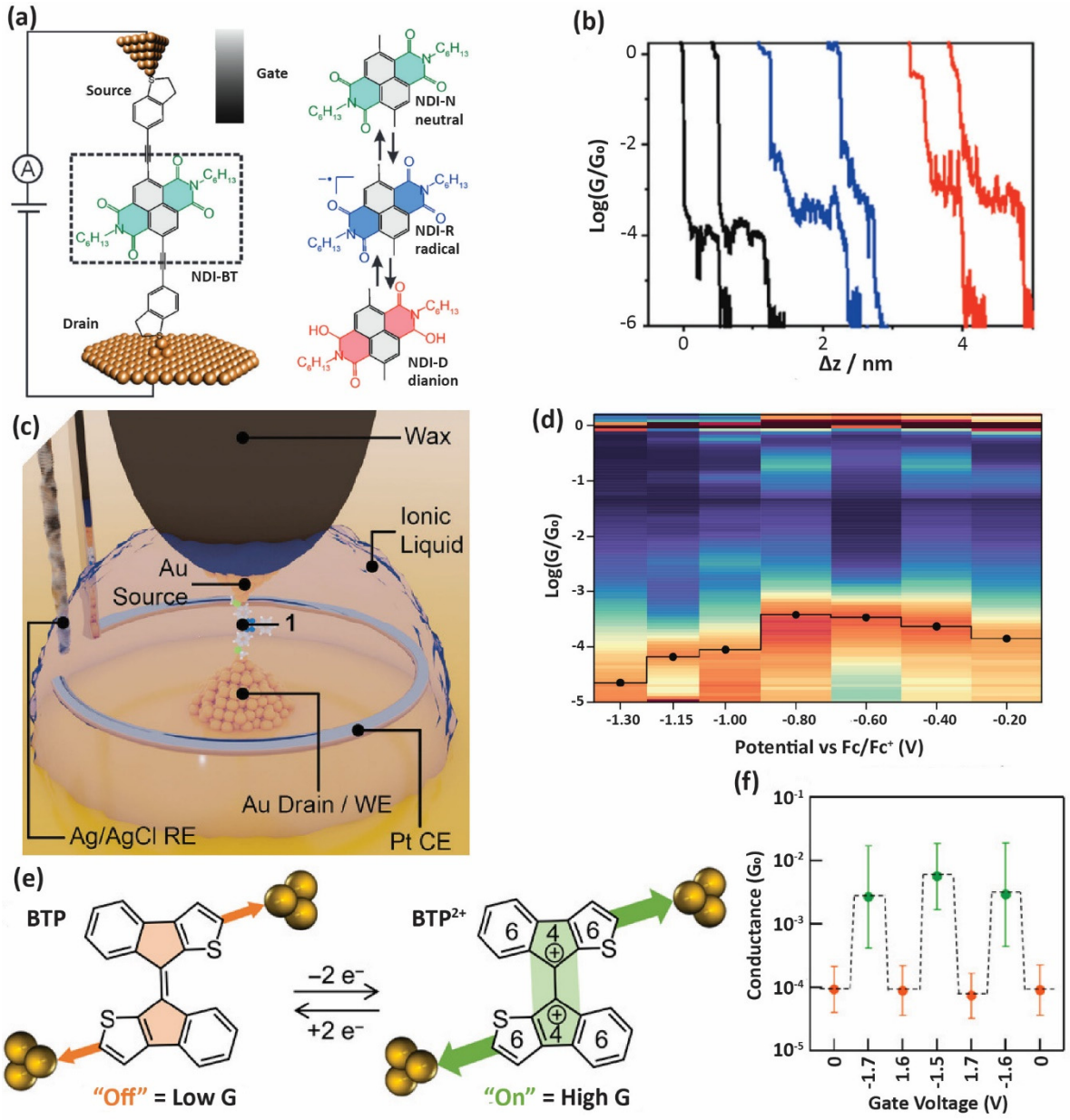

Figure 5. Single-molecule redox reaction in electrochemical break junction. (**a**) Schematic illustration of a redox reaction of naphthalenediimide pendant center via electrochemical gating. (**b**) Traditional conductance vs. distance trace [ND = black, ND^{1-} = blue, ND^{2-} = red]. Figures were reproduced with permission from reference [95]. Copyright 2015, German Chemical Society. (**c**) A four-electrode system of an electrochemical scanning tunneling microscope of a 6-oxoverdazyl radical. (**d**) Heat map of conductance vs. electrochemical potential vs. Fc/Fc+ in 1-butyl-3-methylimidazolium ionic liquid (blue is low count, red is high count). Figures were reproduced with permission from reference [97]. Copyright 2022, German Chemical Society. (**e**) Reversible redox reaction of BTP. (**f**) Alternating low/high conductance vs. gate voltage corresponding to the reversible redox reaction of BTP. Figures were reproduced with permission from reference [98]. Copyright 2017, Science Advances.

6. Conclusions and Outlook

A concerted effort toward pushing the limit of single-molecule technologies has been made to advance electrical detection strategies based on a variety of SMJ techniques. This

effort has enabled direct experimental investigation of chemical reactions at the single-molecule level, allowing one to address inherent ambiguities in bulk chemical reactions. These unprecedented achievements have opened numerous opportunities in key areas like advanced materials, photochemistry, electrochemistry, organometallics, synthetic chemistry, corrosion, and catalysis. In this review, we present representative experimental studies on electric-field-catalyzed chemical reactions, the kinetics of reaction mechanisms, and the evolution of host–guest interactions and redox reactions at the interplay of single-molecule junctions.

As demonstrated in many recent studies, SMJs are now capable of addressing critical chemical questions with a single-molecule resolution. In particular, a directional electric field has been considered a promising tool to alter the outcomes of chemical reactions via controlling and manipulating chemical transition states. To this end, future efforts should be oriented toward expanding the range of reactions that can be tailored by electric fields. In addition, given the remarkable suitability and versatility of the SMJ techniques, attention should also be given to addressing more complex and urgently needed challenges in biological and life sciences, such as DNA sequencing, protein binding, and molecular diagnostics.

Noticeably, new opportunities also emerge when SMJs start to interface with techniques and technologies from other related disciplines [6,27]. For instance, recent efforts in developing novel experimental approaches for exploring plasmonic effect in molecular junctions will pave the path for in-depth understanding of plasmon-driven photocatalysis at the single-molecule level [99,100]. Moreover, experimental attempts in combining Raman spectroscopy directly with an SMJ setup have also successfully enabled simultaneous detection of the electrical and structural information of individual molecules, which charts a path to capture a complete molecular-scale picture of the physical and chemical processes. Therefore, based upon the remarkable progress and new fundamental insights obtained over the past decade, one can reasonably expect that SMJ, as a fertile single-molecule platform bridging gaps of distinct disciplines, will continue to provide solutions to crucial fundamental problems in chemistry, materials science, catalysis, energy, sustainability, and life science.

Author Contributions: Writing—original draft preparation, I.B. and R.T.A.; writing—review and editing, R.T.A., I.B. and K.W.; visualization, I.B. and R.T.A.; supervision, K.W.; project administration, K.W.; funding acquisition, K.W. All authors have read and agreed to the published version of the manuscript.

Funding: This research was funded by U.S. National Science Foundation (Award: OIA-1757220) and Mississippi State University ORED Undergraduate Research Fund.

Data Availability Statement: Data sharing not applicable to this article as no datasets were generated or analyzed during the current study.

Acknowledgments: We thank the support from U.S. National Science Foundation (Award: OIA-1757220) and Mississippi State University ORED Undergraduate Research Fund.

Conflicts of Interest: The authors declare no conflict of interest.

References

1. Chen, H.; Stoddart, F.J. From molecular to supramolecular electronics. *Nat. Rev. Mater.* **2021**, *6*, 804–828. [CrossRef]
2. Stone, I.; Starr, R.L.; Zang, Y.; Nuckolls, C.; Steigerwald, M.L.; Lambert, T.H.; Roy, X.; Venkataraman, L. A single-molecule blueprint for synthesis. *Nat. Rev. Chem.* **2021**, *5*, 695–710. [CrossRef]
3. Liu, K.; Wang, X.; Wang, F. Probing charge transport of ruthenium-complex-based molecular wires at the single-molecule level. *ACS Nano* **2008**, *2*, 2315–2323. [CrossRef] [PubMed]
4. Huang, C.; Jevric, M.; Borges, A.; Olsen, S.T.; Hamill, J.M.; Zheng, J.T.; Yang, Y.; Rudnev, A.; Baghernejad, M.; Broekmann, P.; et al. Single-molecule detection of dihydroazulene photo-thermal reaction using break junction technique. *Nat. Commun.* **2017**, *8*, 15436. [CrossRef]
5. Aradhya, S.V.; Venkataraman, L. Single-molecule junctions beyond electronic transport. *Nat. Nanotechnol.* **2013**, *8*, 399–410. [CrossRef]

6. Tang, C.; Ayinla, R.T.; Wang, K. Beyond electrical conductance: Progress and prospects in single-molecule junctions. *J. Mater. Chem. C* **2022**, *10*, 13717–13733. [CrossRef]
7. Fu, T.; Frommer, K.; Nuckolls, C.; Venkataraman, L. Single-Molecule Junction Formation in Break-Junction Measurements. *J. Phys. Chem. Lett.* **2021**, *12*, 10802–10807. [CrossRef]
8. Xu, B.; Tao, N.J. Measurement of single-molecule resistance by repeated formation of molecular junctions. *Science* **2003**, *301*, 1221–1223. [CrossRef]
9. Wang, K.; Xu, B. Modulation and control of charge transport through single-molecule junctions. *Top. Curr. Chem.* **2017**, *375*, 17. [CrossRef]
10. Giessibl, F.J. Advances in atomic force microscopy. *Rev. Mod. Phys.* **2003**, *75*, 949. [CrossRef]
11. Morita, T.; Lindsay, S. Determination of single molecule conductances of alkanedithiols by conducting-atomic force microscopy with large gold nanoparticles. *J. Am. Chem. Soc.* **2007**, *129*, 7262–7263. [CrossRef] [PubMed]
12. Hamill, J.M.; Wang, K.; Xu, B. Characterizing molecular junctions through the mechanically controlled break-junction approach. *Rep. Electrochem.* **2014**, *4*, 1–11.
13. Xiang, D.; Jeong, H.; Lee, T.; Mayer, D. Mechanically controllable break junctions for molecular electronics. *Adv. Mater.* **2013**, *25*, 4845–4867. [CrossRef]
14. Simmons, J.G. Generalized formula for the electric tunnel effect between similar electrodes separated by a thin insulating film. *J. Appl. Phys.* **1963**, *34*, 1793–1803. [CrossRef]
15. Tsutsui, M.; Taniguchi, M. Single molecule electronics and devices. *Sensors* **2012**, *12*, 7259–7298. [CrossRef] [PubMed]
16. Cao, Y.; Dong, S.; Liu, S.; Liu, Z.; Guo, X. Toward functional molecular devices based on graphene–molecule junctions. *Angew. Chem. Int. Ed.* **2013**, *52*, 3906–3910. [CrossRef]
17. Abbassi, M.E.; Sangtarash, S.; Liu, X.; Perrin, M.L.; Braun, O.; Lambert, C.; van der Zant, H.S.J.; Yitzchaik, S.; Decurtins, S.; Liu, S.-X. Robust graphene-based molecular devices. *Nat. Nanotechnol.* **2019**, *14*, 957–961. [CrossRef]
18. Yang, C.; Qin, A.; Tang, B.Z.; Guo, X. Fabrication and functions of graphene–molecule–graphene single-molecule junctions. *J. Chem. Phys.* **2020**, *152*, 120902. [CrossRef] [PubMed]
19. Binnig, G.; Rohrer, H.; Gerber, C.; Weibel, E. Tunneling through a controlled vacuum gap. *Appl. Phys. Lett.* **1982**, *40*, 178–180.
20. Hirjibehedin, C.F.; Wang, Y. Recent advances in scanning tunneling microscopy and spectroscopy. *J. Phys. Condens. Matter* **2014**, *26*, 390301. [CrossRef]
21. Liu, X.-W.; Stamp, A.P. Theory of scanning tunneling microscopy. *J. Vac. Sci. Technol. B* **1994**, *12*, 2189–2192. [CrossRef]
22. Chakraborty, I.; Bodurtha, K.J.; Heeder, N.J.; Godfrin, M.P.; Tripathi, A.; Hurt, R.H.; Shukla, A.; Bose, A. Massive electrical conductivity enhancement of multilayer graphene/polystyrene composites using a nonconductive filler. *ACS Appl. Mater. Interfaces* **2014**, *6*, 16472–16475. [CrossRef] [PubMed]
23. Li, Y.; Yang, C.; Guo, X. Single-molecule electrical detection: A promising route toward the fundamental limits of chemistry and life science. *Acc. Chem. Res.* **2019**, *53*, 159–169. [CrossRef]
24. Stuyver, T.; Danovich, D.; Joy, J.; Shaik, S. External electric field effects on chemical structure and reactivity. *Comput. Mol. Sci.* **2020**, *10*, e1438. [CrossRef]
25. Xie, X.; Li, P.; Xu, Y.; Zhou, L.; Yan, Y.; Xie, L.; Jia, C.; Guo, X. Single-molecule junction: A reliable platform for monitoring molecular physical and chemical processes. *ACS Nano* **2022**, *16*, 3476–3505. [CrossRef]
26. Yu, P.; Feng, A.; Zhao, S.; Wei, J.; Yang, Y.; Shi, J.; Hong, W. Recent progress of break junction technique in single-molecule reaction chemistry. *Acta Phys.-Chim. Sin.* **2019**, *35*, 829–839. [CrossRef]
27. Zhang, H.; Shiri, M.; Ayinla, R.T.; Qiang, Z.; Wang, K. Switching the conductance of a single molecule: Lessons from molecular junctions. *MRS Commun.* **2022**, *12*, 495–509. [CrossRef]
28. Su, T.A.; Neupane, M.; Steigerwald, M.L.; Venkataraman, L.; Nuckolls, C. Chemical principles of single-molecule electronics. *Nat. Rev. Mater.* **2016**, *1*, 16002. [CrossRef]
29. Sun, L.; Diaz-Fernandez, Y.A.; Gschneidtner, T.A.; Westerlund, F.; Lara-Avila, S.; Moth-Poulsen, K. Single-molecule electronics: From chemical design to functional devices. *Chem. Soc. Rev.* **2014**, *43*, 7378–7411. [CrossRef]
30. Aragones, A.C.; Haworth, N.L.; Darwish, N.; Ciampi, S.; Bloomfield, N.J.; Wallace, G.G.; Diez-Perez, I.; Coote, M.L. Electrostatic catalysis of a diels–alder reaction. *Nature* **2016**, *531*, 88–91. [CrossRef]
31. Quintans, C.; Andrienko, D.; Domke, K.F.; Aravena, D.; Koo, S.; Díez-Pérez, I.; Aragonès, A.C. Tuning single-molecule conductance by controlled electric field-induced trans-to-cis isomerisation. *Appl. Sci.* **2021**, *11*, 3317. [CrossRef]
32. Tang, C.; Shiri, M.; Zhang, H.; Ayinla, R.T.; Wang, K. Light-driven charge transport and optical sensing in molecular junctions. *Nanomaterials* **2022**, *12*, 698. [CrossRef]
33. Zhou, J.; Wang, K.; Xu, B.; Dubi, Y. Photoconductance from exciton binding in molecular junctions. *J. Am. Chem. Soc.* **2018**, *140*, 70–73. [CrossRef] [PubMed]
34. Li, X.; Hu, D.; Tan, Z.; Bai, J.; Xiao, Z.; Yang, Y.; Shi, J.; Hong, W. Supramolecular systems and chemical reactions in single-molecule break junctions. *Top. Curr. Chem.* **2017**, *375*, 42. [CrossRef]
35. Taniguchi, M. Paving the way to single-molecule chemistry through molecular electronics. *Phys. Chem. Chem. Phys.* **2019**, *21*, 9641–9650. [CrossRef] [PubMed]
36. Shaik, S.; De Visser, S.P.; Kumar, D. External electric field will control the selectivity of enzymatic-like bond activations. *J. Am. Chem. Soc.* **2004**, *126*, 11746–11749. [CrossRef] [PubMed]

37. Shaik, S.; Danovich, D.; Joy, J.; Wang, Z.; Stuyver, T. Electric-field mediated chemistry: Uncovering and exploiting the potential of (oriented) electric fields to exert chemical catalysis and reaction control. *J. Am. Chem. Soc.* **2020**, *142*, 12551–12562. [CrossRef]
38. Vasilev, K.; Doppagne, B.; Neuman, T.; Rosławska, A.; Bulou, H.; Boeglin, A.; Scheurer, F.; Schull, G. Internal Stark effect of single-molecule fluorescence. *Nat. Commun.* **2022**, *13*, 677. [CrossRef]
39. Shaik, S.; Mandal, D.; Ramanan, R. Oriented electric fields as future smart reagents in chemistry. *Nat. Chem.* **2016**, *8*, 1091–1098. [CrossRef]
40. Bhattacharyya, D.; Videla, P.E.; Cattaneo, M.; Batista, V.S.; Lian, T.; Kubiak, C.P. Vibrational Stark shift spectroscopy of catalysts under the influence of electric fields at electrode–solution interfaces. *Chem. Sci.* **2021**, *12*, 10131–10149. [CrossRef]
41. Darwish, N. Chemical mechanisms, one molecule at a time. *Nat. Nanotechnol.* **2021**, *16*, 1176–1177. [CrossRef] [PubMed]
42. Wesley, T.S.; Román-Leshkov, Y.; Surendranath, Y. Spontaneous electric fields play a key role in thermochemical catalysis at metal−liquid interfaces. *ACS Cent. Sci.* **2021**, *7*, 1045–1055. [CrossRef] [PubMed]
43. Meir, R.; Chen, H.; Lai, W.; Shaik, S. Oriented electric fields accelerate Diels–Alder reactions and control the endo/exo selectivity. *ChemPhysChem* **2010**, *11*, 301–310. [CrossRef]
44. Zang, Y.; Zou, Q.; Fu, T.; Ng, F.; Fowler, B.; Yang, J.; Li, H.; Steigerwald, M.L.; Nuckolls, C.; Venkataraman, L. Directing isomerization reactions of cumulenes with electric fields. *Nat. Commun.* **2019**, *10*, 4482. [CrossRef]
45. Huang, X.; Tang, C.; Li, J.; Chen, L.-C.; Zheng, J.; Zhang, P.; Le, J.; Li, R.; Li, X.; Liu, J. Electric field–induced selective catalysis of single-molecule reaction. *Sci. Adv.* **2019**, *5*, eaaw3072. [CrossRef]
46. Wen, H.; Li, W.; Chen, J.; He, G.; Li, L.; Olson, M.A.; Sue, A.C.-H.; Stoddart, J.F.; Guo, X. Complex formation dynamics in a single-molecule electronic device. *Sci. Adv.* **2016**, *2*, e1601113. [CrossRef] [PubMed]
47. Guo, Y.; Yang, C.; Li, H.; Zhang, L.; Zhou, S.; Zhu, X.; Fu, H.; Li, Z.; Liu, Z.; Jia, C. Accurate Single-Molecule Kinetic Isotope Effects. *J. Am. Chem. Soc.* **2022**, *144*, 3146–3153. [CrossRef] [PubMed]
48. Guan, J.; Jia, C.; Li, Y.; Liu, Z.; Wang, J.; Yang, Z.; Gu, C.; Su, D.; Houk, K.N.; Zhang, D. Direct single-molecule dynamic detection of chemical reactions. *Sci. Adv.* **2018**, *4*, eaar2177. [CrossRef]
49. Zhou, C.; Li, X.; Gong, Z.; Jia, C.; Lin, Y.; Gu, C.; He, G.; Zhong, Y.; Yang, J.; Guo, X. Direct observation of single-molecule hydrogen-bond dynamics with single-bond resolution. *Nat. Commun.* **2018**, *9*, 807. [CrossRef]
50. Yang, C.; Liu, Z.; Li, Y.; Zhou, S.; Lu, C.; Guo, Y.; Ramirez, M.; Zhang, Q.; Li, Y.; Liu, Z. Electric field–catalyzed single-molecule diels-alder reaction dynamics. *Sci. Adv.* **2021**, *7*, eabf0689. [CrossRef]
51. Jia, C.; Migliore, A.; Xin, N.; Huang, S.; Wang, J.; Yang, Q.; Wang, S.; Chen, H.; Wang, D.; Feng, B. Covalently bonded single-molecule junctions with stable and reversible photoswitched conductivity. *Science* **2016**, *352*, 1443–1445. [CrossRef] [PubMed]
52. Hooshmand, S.E.; Heidari, B.; Sedghi, R.; Varma, R.S. Recent advances in the Suzuki–Miyaura cross-coupling reaction using efficient catalysts in eco-friendly media. *Green Chem.* **2019**, *21*, 381–405. [CrossRef]
53. Han, F.-S. Transition-metal-catalyzed suzuki–miyaura cross-coupling reactions: A remarkable advance from palladium to nickel catalysts. *Chem. Soc. Rev.* **2013**, *42*, 5270–5298. [CrossRef] [PubMed]
54. D'Alterio, M.C.; Casals-Cruañas, È.; Tzouras, N.V.; Talarico, G.; Nolan, S.P.; Poater, A. mechanistic aspects of the palladium-catalyzed suzuki-miyaura cross-coupling reaction. *Chem.-Eur. J.* **2021**, *27*, 13481–13493. [CrossRef] [PubMed]
55. Wang, C.; Glorius, F. Controlled iterative cross-coupling: On the way to the automation of organic synthesis. *Angew. Chem. Int. Ed.* **2009**, *48*, 5240–5244. [CrossRef]
56. Dobrounig, P.; Trobe, M.; Breinbauer, R. Sequential and iterative pd-catalyzed cross-coupling reactions in organic synthesis. *Mon. Chem.-Chem. Mon.* **2017**, *148*, 3–35. [CrossRef]
57. Boisjan, A.; Allemann, C.; Fadini, L. Impact of solvent and their contaminants on pd/c catalyzed suzuki-miyaura cross-coupling reactions. *Helv. Chim. Acta* **2021**, *104*, e2100035.
58. Yang, C.; Zhang, L.; Lu, C.; Zhou, S.; Li, X.; Li, Y.; Yang, Y.; Li, Y.; Liu, Z.; Yang, J.; et al. Unveiling the full reaction path of the suzuki–miyaura cross-coupling in a single-molecule junction. *Nat. Nanotechnol.* **2021**, *16*, 1214–1223. [CrossRef]
59. Ma, X.; Zhao, Y. Biomedical applications of supramolecular systems based on host–guest interactions. *Chem. Rev.* **2015**, *115*, 7794–7839. [CrossRef]
60. Hu, Q.D.; Tang, G.P.; Chu, P.K. Cyclodextrin-based host–guest supramolecular nanoparticles for delivery: From design to applications. *Acc. Chem. Res.* **2014**, *47*, 2017–2025. [CrossRef]
61. Yang, K.; Zhang, Z.; Du, J.; Li, W.; Pei, Z. Host–guest interaction based supramolecular photodynamic therapy systems: A promising candidate in the battle against cancer. *Chem. Commun.* **2020**, *56*, 5865–5876. [CrossRef] [PubMed]
62. Rizzi, V.; Bonati, L.; Ansari, N.; Parrinello, M. The role of water in host-guest interaction. *Nat. Commun.* **2021**, *12*, 93. [CrossRef] [PubMed]
63. Qu, D.H.; Wang, Q.C.; Zhang, Q.W.; Ma, X.; Tian, H. Photoresponsive host–guest functional systems. *Chem. Rev.* **2015**, *115*, 7543–7588. [CrossRef] [PubMed]
64. Loh, X.J. Supramolecular host–guest polymeric materials for biomedical applications. *Mater. Horiz.* **2014**, *1*, 185–195. [CrossRef]
65. Li, J.; Qian, Y.; Duan, W.; Zeng, Q. Advances in the study of the host-guest interaction by using coronene as the guest molecule. *Chin. Chem. Lett.* **2019**, *30*, 292–298. [CrossRef]
66. Wankar, J.; Kotla, N.G.; Gera, S.; Rasala, S.; Pandit, A.; Rochev, Y.A. Recent advances in host–guest self-assembled cyclodextrin carriers: Implications for responsive drug delivery and biomedical engineering. *Adv. Funct. Mater.* **2020**, *30*, 1909049. [CrossRef]

67. Milan, D.C.; Krempe, M.; Ismael, A.K.; Movsisyan, L.D.; Franz, M.; Grace, I.; Brooke, R.J.; Schwarzacher, W.; Higgins, S.J.; Anderson, H.L. The single-molecule electrical conductance of a rotaxane-hexayne supramolecular assembly. *Nanoscale* **2017**, *9*, 355–361. [CrossRef]
68. Yuan, S.; Qian, Q.; Zhou, Y.; Zhao, S.; Lin, L.; Duan, P.; Xu, X.; Shi, J.; Xu, W.; Feng, A.; et al. Tracking confined reaction based on host–guest interaction using single-molecule conductance measurement. *Small* **2022**, *18*, 2104554. [CrossRef]
69. Zhang, W.; Gan, S.; Vezzoli, A.; Davidson, R.J.; Milan, D.C.; Luzyanin, K.V.; Higgins, S.J.; Nichols, R.J.; Beeby, A.; Low, P.J. Single-molecule conductance of viologen–cucurbit [8] uril host–guest complexes. *ACS Nano* **2016**, *10*, 5212–5220. [CrossRef]
70. Nichols, R.J.; Higgins, S.J. Single molecule electrochemistry in nanoscale junctions. *Curr. Opin. Electrochem.* **2017**, *4*, 98–104. [CrossRef]
71. Nichols, R.J.; Higgins, S.J. Single molecule nanoelectrochemistry in electrical junctions. *Acc. Chem. Res.* **2016**, *49*, 2640–2648. [CrossRef] [PubMed]
72. Li, Z.; Li, H.; Chen, S.; Froehlich, T.; Yi, C.; SchÖnenberger, C.; Calame, M.; Decurtins, S.; Liu, S.-X.; Borguet, E. Regulating a benzodifuran single molecule redox switch via electrochemical gating and optimization of molecule/electrode coupling. *J. Am. Chem. Soc.* **2014**, *136*, 8867–8870. [CrossRef] [PubMed]
73. Leary, E.; Higgins, S.J.; van Zalinge, H.; Haiss, W.; Nichols, R.J.; Nygaard, S.; Jeppesen, J.O.; Ulstrup, J. Structure-property relationships in redox-gated single molecule junctions-a comparison of pyrrolo-tetrathiafulvalene and viologen redox groups. *J. Am. Chem. Soc.* **2008**, *130*, 12204–12205. [CrossRef] [PubMed]
74. de Nijs, B.; Benz, F.; Barrow, S.J.; Sigle, D.O.; Chikkaraddy, R.; Palma, A.; Carnegie, C.; Kamp, M.; Sundararaman, R.; Narang, P. Plasmonic tunnel junctions for single-molecule redox chemistry. *Nat. Commun.* **2017**, *8*, 994. [CrossRef] [PubMed]
75. Nichols, R.J.; Higgins, S.J. Single-molecule electronics: Chemical and analytical perspectives. *Annu. Rev. Anal. Chem.* **2015**, *8*, 389–417. [CrossRef] [PubMed]
76. Lambert, C. Basic concepts of quantum interference and electron transport in single-molecule electronics. *Chem. Soc. Rev.* **2015**, *44*, 875–888. [CrossRef]
77. Kuznetsov, A.M.; Ulstrup, J. Mechanisms of in situ scanning tunnelling microscopy of organized redox molecular assemblies. *J. Phys. Chem. A* **2000**, *104*, 11531–11540. [CrossRef]
78. Haiss, W.; van Zalinge, H.; Higgins, S.J.; Bethell, D.; Höbenreich, H.; Schiffrin, D.J.; Nichols, R.J. Redox state dependence of single molecule conductivity. *J. Am. Chem. Soc.* **2003**, *125*, 15294–15295. [CrossRef]
79. Haiss, W.; Albrecht, T.; Van Zalinge, H.; Higgins, S.; Bethell, D.; Höbenreich, H.; Schiffrin, D.; Nichols, R.J.; Kuznetsov, A.M.; Zhang, J.; et al. Single-molecule conductance of redox molecules in electrochemical scanning tunneling microscopy. *J. Phys. Chem. B* **2007**, *111*, 6703–6712. [CrossRef]
80. Zhang, J.; Kuznetsov, A.M.; Medvedev, I.G.; Chi, Q.; Albrecht, T.; Jensen, P.S.; Ulstrup, J. Single-molecule electron transfer in electrochemical environments. *Chem. Rev.* **2008**, *108*, 2737–2791. [CrossRef]
81. Ward, J.S.; Vezzoli, A. Key advances in electrochemically-addressable single-molecule electronics. *Curr. Opin. Electrochem.* **2022**, *35*, 101083. [CrossRef]
82. Kuznetsov, A.M.; Ulstrup, J. Single-molecule electron tunnelling through multiple redox levels with environmental relaxation. *J. Electroanal. Chem.* **2004**, *564*, 209–222. [CrossRef]
83. Gittins, D.I.; Bethell, D.; Schiffrin, D.J.; Nichols, R.J. A nanometre-scale electronic switch consisting of a metal cluster and redox-addressable groups. *Nature* **2000**, *408*, 67–69. [CrossRef] [PubMed]
84. Hines, T.; Díez-Pérez, I.; Nakamura, H.; Shimazaki, T.; Asai, Y.; Tao, N. Controlling formation of single-molecule junctions by electrochemical reduction of diazonium terminal groups. *J. Am. Chem. Soc.* **2013**, *135*, 3319–3322. [CrossRef] [PubMed]
85. Alessandrini, A.; Salerno, M.; Frabboni, S.; Facci, P. Single-metalloprotein wet biotransistor. *Appl. Phys. Lett.* **2005**, *86*, 133902. [CrossRef]
86. Davis, J.J.; Peters, B.; Xi, W. Force modulation and electrochemical gating of conductance in a cytochrome. *J. Phys. Condens. Matter* **2008**, *20*, 374123. [CrossRef]
87. Zhang, J.; Chi, Q.; Hansen, A.G.; Jensen, P.S.; Salvatore, P.; Ulstrup, J. Interfacial electrochemical electron transfer in biology-towards the level of the single molecule. *FEBS Lett.* **2012**, *586*, 526–535. [CrossRef]
88. Diez-Perez, I.; Li, Z.; Hihath, J.; Li, J.; Zhang, C.; Yang, X.; Zang, L.; Dai, Y.; Feng, X.; Muellen, K.; et al. Gate-controlled electron transport in coronenes as a bottom-up approach towards graphene transistors. *Nat. Commun.* **2010**, *1*, 31. [CrossRef]
89. Tao, S.; Zhang, Q.; Vezzoli, A.; Zhao, C.; Zhao, C.; Higgins, S.J.; Smogunov, A.; Dappe, Y.J.; Nichols, R.J.; Yang, L. Electrochemical gating for single-molecule electronics with hybrid Au | graphene contacts. *Phys. Chem. Chem. Phys.* **2022**, *24*, 6836–6844. [CrossRef]
90. Wu, C.; Qiao, X.; Robertson, C.M.; Higgins, S.J.; Cai, C.; Nichols, R.J.; Vezzoli, A. A chemically soldered polyoxometalate single-molecule transistor. *Angew. Chem. Int. Ed.* **2020**, *132*, 12127–12132. [CrossRef]
91. Li, X.; Hihath, J.; Chen, F.; Masuda, T.; Zang, L.; Tao, N. Thermally activated electron transport in single redox molecules. *J. Am. Chem. Soc.* **2007**, *129*, 11535–11542. [CrossRef]
92. Li, C.; Mishchenko, A.; Li, Z.; Pobelov, I.; Wandlowski, T.; Li, X.-Q.; Würthner, F.; Bagrets, A.; Evers, F. Electrochemical gate-controlled electron transport of redox-active single perylene bisimide molecular junctions. *J. Phys. Condens. Matter* **2008**, *20*, 374122. [CrossRef] [PubMed]

93. Diez-Perez, I.; Li, Z.; Guo, S.; Madden, C.; Huang, H.; Che, Y.; Yang, X.; Zang, L.; Tao, N. Ambipolar transport in an electrochemically gated single-molecule field-effect transistor. *ACS Nano* **2012**, *6*, 7044–7052. [CrossRef] [PubMed]
94. Xiao, X.; Brune, D.; He, J.; Lindsay, S.; Gorman, C.B.; Tao, N. Redox-gated electron transport in electrically wired ferrocene molecules. *Chem. Phys.* **2006**, *326*, 138–143. [CrossRef]
95. Li, Y.; Baghernejad, M.; Qusiy, A.G.; Zsolt Manrique, D.; Zhang, G.; Hamill, J.; Fu, Y.; Broekmann, P.; Hong, W.; Wandlowski, T.; et al. Three-state single-molecule naphthalenediimide switch: Integration of a pendant redox unit for conductance tuning. *Angew. Chem. Int. Ed.* **2015**, *127*, 13790–13793. [CrossRef]
96. Chen, H.; Brasiliense, V.; Mo, J.; Zhang, L.; Jiao, Y.; Chen, Z.; Jones, L.O.; He, G.; Guo, Q.-H.; Chen, X.-Y.; et al. Single-molecule charge transport through positively charged electrostatic anchors. *J. Am. Chem. Soc.* **2021**, *143*, 2886–2895. [CrossRef]
97. Naghibi, S.; Sangtarash, S.; Kumar, V.J.; Wu, J.-Z.; Judd, M.M.; Qiao, X.; Gorenskaia, E.; Higgins, S.J.; Cox, N.; Nichols, R.J.; et al. Redox-addressable single-molecule junctions incorporating a persistent organic radical. *Angew. Chem. Int. Ed.* **2022**, *61*, e202116985. [CrossRef]
98. Yin, X.; Zang, Y.; Zhu, L.; Low, J.Z.; Liu, Z.-F.; Cui, J.; Neaton, J.B.; Venkataraman, L.; Campos, L.M. A reversible single-molecule switch based on activated antiaromaticity. *Sci. Adv.* **2017**, *3*, eaao2615. [CrossRef]
99. Reddy, H.; Wang, K.; Kudyshev, Z.; Zhu, L.; Yan, S.; Vezzoli, A.; Higgins, S.J.; Gavini, V.; Boltasseva, A.; Reddy, P. Determining plasmonic hot-carrier energy distributions via single-molecule transport measurements. *Science* **2020**, *369*, 423–426. [CrossRef]
100. Wang, M.; Wang, T.; Ojambati, O.S.; Duffin, T.J.; Kang, K.; Lee, T.; Scheer, E.; Xiang, D.; Nijhuis, C.A. Plasmonic phenomena in molecular junctions: Principles and applications. *Nat. Rev. Chem.* **2022**, *6*, 681–704. [CrossRef]